Journal of Pharmacological Sciences 153 (2023) 104–112

Contents lists available at ScienceDirect

Journal of Pharmacological Sciences

journal homepage: www.elsevier.com/locate/jphs

Full Paper

CYP11A1 silencing suppresses HMGCR expression via cholesterol accumulation and sensitizes CRPC cell line DU-145 to atorvastatin

Jiro Tashiro [a], Akihiro Sugiura [a], Tomoko Warita [b], Nanami Irie [c], Danang Dwi Cahyadi [a], Takuro Ishikawa [d, e, *], Katsuhiko Warita [a, e, **]

[a] Department of Veterinary Anatomy, Joint Graduate School of Veterinary Sciences, Tottori University, Tottori, Japan
[b] Department of Biomedical Sciences, School of Biological and Environmental Sciences, Kwansei Gakuin University, Hyogo, Japan
[c] Graduate School of Science and Technology, Kwansei Gakuin University, Hyogo, Japan
[d] Department of Anatomy, School of Medicine, Aichi Medical University, Aichi, Japan
[e] Joint Department of Veterinary Medicine, Tottori University, Tottori, Japan

ARTICLE INFO

Article history:
Received 10 April 2023
Received in revised form
7 August 2023
Accepted 17 August 2023
Available online 23 August 2023

Keywords:
Statin
CRPC
HMGCR
Cholesterol
EMT

ABSTRACT

Statins, which are cholesterol synthesis inhibitors, are well-known therapeutics for dyslipidemia; however, some studies have anticipated their use as anticancer agents. However, epithelial cancer cells show strong resistance to statins through an increased expression of HMG-CoA reductase (HMGCR), an inhibitory target of statins. Castration-resistant prostate cancer (CRPC) cells synthesize androgens from cholesterol on their own. We performed suppression of CYP11A1, a rate-limiting enzyme in androgen synthesis from cholesterol, using siRNA or inhibitors, to examine the effect of steroidogenesis inhibition on statin sensitivity in CRPC cells. Here, we suggested that CYP11A1 silencing sensitized the statin-resistant CRPC cell line DU-145 to atorvastatin via HMGCR downregulation by an increase in intracellular free cholesterol. We further demonstrated that CYP11A1 silencing induced epithelial-mesenchymal transition, which converted DU-145 cells into a statin-sensitive phenotype. This suggests that concomitant use of CYP11A1 inhibitors could be an effective approach for overcoming statin resistance in CRPC. Moreover, we showed that ketoconazole, a CYP11A1 inhibitor, sensitized DU-145 cells to atorvastatin, although not all the molecular events observed in CYP11A1 silencing were reproducible. Although further studies are necessary to clarify the detailed mechanisms, ketoconazole may be effective as a concomitant drug that potentiates the anticancer effect of atorvastatin.

1. Introduction

Statins are inhibitors of 3-hydroxy-3-methylglutaryl coenzyme A reductase (HMGCR), a rate-limiting enzyme of the mevalonate pathway, and are used to treat cerebro-cardiovascular diseases.[1] Recent studies have demonstrated that statins also exert anticancer effects by inhibiting the proliferation, migration, invasion, metastasis formation, and angiogenesis, and by inducing apoptosis and autophagy in many types of cancers, and has attracted attention as a repurposed agent for cancer treatment.[1,2] However, the degree of growth inhibition by statins varies depending on the cancer phenotype. While statins effectively suppress the growth of mesenchymal cancer cells lacking functional E-cadherin, epithelial cancer cells expressing E-cadherin on plasma membrane are less sensitive to statins.[3–5] The presence of statin-resistant cancer cells is challenging for the use of statins in cancer therapy.

Statin treatment induces an increase in HMGCR and other enzymes related to the mevalonate pathway in cancer cells, which is considered one of the mechanisms underlying resistance to statins.[6–9] Conversely, inhibition of HMGCR expression sensitizes several cancer cell types to statins.[8,10,11] Hence, HMGCR downregulation is an attractive approach to overcome statin resistance in cancer cells. HMGCR expression is controlled by intermediate metabolites, final products, and derivatives of the mevalonate pathway at the transcriptional and post-transcriptional levels.[12,13] For instance, cholesterol, the end product of the mevalonate pathway,

* Corresponding author.
** Corresponding author.
E-mail addresses: ishikawa.takuro.349@mail.aichi-med-u.ac.jp (T. Ishikawa), waritak@tottori-u.ac.jp (K. Warita).
Peer review under responsibility of Japanese Pharmacological Society.

https://doi.org/10.1016/j.jphs.2023.08.002

inhibits activation of sterol regulatory element-binding protein 2 (SREBP2), an HMGCR transcription factor, resulting in decreased HMGCR expression.[12,14,15]

Epithelial-mesenchymal transition (EMT) is a complex process that increases invasiveness and metastatic activity of cancer cells.[16] Cells undergoing EMT are characterized by a decrease in cell adhesion biomarkers, such as E-cadherin, claudin, and cytokeratin, and an increase in mesenchymal cell biomarkers, including vimentin, fibronectin, and N-cadherin.[16,17] EMT induces drug resistance in cancer cells.[17] In contrast, epithelial cancer cells undergoing transforming growth factor-β (TGF-β)-induced EMT showed attenuated HMGCR upregulation and increased sensitivity to atorvastatin treatment.[11]

Prostate cancer was reported as the second most common cancer following lung cancer in males in 2020; it is one of the main causes of cancer-related deaths.[18] Prostate cancer progression depends on the androgen receptor signaling activated by androgens, which are mainly secreted in the testes.[19,20] Therefore, androgen deprivation therapy (ADT), including surgical and medical castration, is the first choice of treatment for patients with advanced prostate cancer.[19,20] However, most prostate cancers acquire resistance to treatment and relapse several years later. These cancers are known as castration-resistant prostate cancer (CRPC).[20,21] It has been reported that some prostate cancer cells synthesize androgens from cholesterol on their own.[22] Furthermore, *de novo* androgen synthesis may be one of the mechanisms underlying CRPC progression, as several studies have shown that the expression of steroidogenic enzymes is increased in CRPC.[23,24] The conversion of cholesterol to pregnenolone, the rate-limiting step in *de novo* androgen synthesis, is catalyzed by the cholesterol side chain cleavage enzyme CYP11A1.[22,23]

Here, we investigated the effect of CYP11A1 suppression on statin sensitivity in CRPC cells and the mechanisms underlying this effect in terms of cholesterol metabolism and EMT. We demonstrated that CYP11A1 silencing sensitized statin-resistant CRPC cell line, DU-145, to atorvastatin by reducing HMGCR expression and increasing intracellular free cholesterol. Moreover, we showed that CYP11A1 silencing induced EMT in DU-145 cells, resulting in a statin-sensitive mesenchymal-like phenotype.

2. Materials and methods

2.1. Cell culture

Two human prostate cancer cell lines (DU-145 and LNCaP) that have been reported to synthesize androgens *de novo* on their own were used.[22] Cells were cultured in RPMI 1640 medium (Thermo Fisher Scientific, Waltham, MA, USA) supplemented with 10% heat-inactivated fetal bovine serum (FBS; Biosera, Boussens, France) and penicillin (100 U/mL)/streptomycin (100 μg/mL) (Fujifilm Wako Pure Chemical, Osaka, Japan) in 5% CO_2 humidity incubator at 37 °C. For siRNA experiments, RPMI 1640 medium containing only 10% FBS was used.

2.2. CYP11A1 silencing

For targeted gene silencing, pre-designed siRNA oligonucleotides specific for CYP11A1 (NM_000781.2, NM_001099773.1, siRNA ID#s3866, targeted exon 4, siRNA location: 968, 1042, Thermo Fisher Scientific) were used. Silencer negative control siRNA (#4390843, Thermo Fisher Scientific) was used as a negative control. Reverse transfections were conducted in 12-well plates (6.0×10^4 cells/mL) according to the manufacturer's instructions using Lipofectamine RNAiMAX (Thermo Fisher Scientific), FBS/antibiotic-free RPMI 1640, and siRNAs (final concentration, 10 nM) for the respective targets. After 72 h of transfection, the knockdown efficiency was confirmed using real-time PCR.

2.3. Real-time PCR

Total cellular RNA was extracted using ISOSPIN Cell & Tissue RNA kit (Nippon Gene, Tokyo, Japan). cDNA synthesis was performed using ReverTra Ace qPCR RT Master Mix (Toyobo, Osaka, Japan). Sequences of the primer sets used for real-time PCR are shown in Supplementary Table S1. Real-time PCR was conducted using LightCycler FastStart DNA MasterPLUS SYBR Green I mix and LightCycler rapid thermal cycler system (Roche Diagnostics, Lewes, UK).

2.4. Western blotting

Western blotting was performed as previously reported with some modifications.[11] Briefly, protein lysates were extracted with CelLytic M (Sigma-Aldrich, St. Louis, MO, USA) supplemented with Halt Protease and Phosphatase Inhibitor Single-Use Cocktail, EDTA-Free (Thermo Fisher Scientific). The separated protein (3–10 μg) was transferred to a nitrocellulose membrane. After blocking with 5% skim milk (Morinaga Milk industry, Tokyo, Japan) for 1–12 h, the membranes were probed with the following primary antibodies for 1–12 h: anti-HMGCR mouse monoclonal antibody (1:1000 dilution, AMab90618; Atlas, Cambridge, UK), anti-SREBP2 mouse monoclonal antibody (1:250 dilution, 557037; BD Biosciences, San Diego, CA, USA), anti-E-cadherin rabbit monoclonal antibody (1:1000 dilution, 24E10; Cell Signaling Technology, Beverly, MA, USA), anti-vimentin mouse monoclonal antibody (1:1000 dilution, 5G3F10; Cell Signaling Technology), and anti-fibronectin antibody (1:1000 dilution, ab2413; Abcam, Cambridge, UK). Glyceraldehyde 3-phosphate dehydrogenase (GAPDH) protein level (loading control) was determined using anti-GAPDH rabbit monoclonal antibody (1:2000 dilution, 14C10; Cell Signaling Technology). After probing, the membranes were washed and incubated with horseradish peroxidase (HRP)-labeled anti-mouse IgG goat antibody (R&D Systems, Minneapolis, MN, USA) or anti-rabbit IgG goat antibody (SeraCare, Milford, MA, USA) for 1 h. After washing, the membranes were incubated with the detection reagent Clarity Western enhanced chemiluminescence (ECL) substrate (Bio-Rad) for 2–5 min. Protein signals were visualized using C-DiGit Blot Scanner (Li-Cor Biosciences, Lincoln, NE, USA). Signals were quantified using the Image Studio software (Li-Cor Biosciences) and standardized according to GAPDH protein level.

2.5. Lipid extraction and free cholesterol quantification

Cells cultured in 12-well plates were trypsinized and washed thrice with phosphate-buffered saline (PBS). The frozen cell pellets (−80 °C) were sonicated in lysis buffer (chloroform: isopropanol: NP-40 Substitute [Fujifilm Wako Pure Chemical] = 7: 11: 0.1). The cell lysates were centrifuged at 16,000×*g* at 4 °C for 10 min, and the supernatants were collected. The lysates were heated at 50 °C, and organic solvents were removed under vacuum. Dried lipids were sonicated in the assay diluent. Cellular free cholesterol levels were measured using Total Cholesterol Assay Kit (Colorimetric, STA-384; Cell Biolabs, San Diego, CA, USA) according to the manufacturer's instructions. Free cholesterol content was normalized to the cell number and volume.

2.6. Filipin III staining

Cells cultured on coverslips in 24-well plates were fixed for 30 min at room temperature with 2% paraformaldehyde (Nacalai

Tesque, Tokyo, Japan). After three PBS washes, cells were incubated with 50 μg/mL Filipin III (Cayman Chemical, Ann Arbor, MI, USA) in the dark at room temperature for 1 h. Coverslips were mounted on Fluoromount/Plus (Diagnostic Biosystems, Pleasanton, CA, USA) after being washed twice with PBS. Images were obtained using a fluorescent microscope (DP71, Olympus, Tokyo, Japan). Fluorescent intensity was quantified using the ImageJ software (National Institutes of Health, Bethesda, MD, USA).

2.7. Cell viability assay and IC_{50} determination

Cells were seeded in 96-well plates at a density of 2.5×10^4 cells/mL. The next day, the cells were treated with drugs, including atorvastatin (Sigma-Aldrich), ketoconazole (Fujifilm Wako Pure Chemical), mitotane (o,p'-DDD standard; Fujifilm Wako Pure Chemical), and aminoglutethimide (Fujifilm Wako Pure Chemical). The cells were co-treated with atorvastatin and siRNA without pre-culture. After incubation for 72 h, cell viability was assessed using Cell Counting Kit-8 (CCK-8; Dojindo Laboratories, Kumamoto, Japan). IC_{50} concentrations were determined by fitting the data to dose-response curves using the ImageJ software. To confirm the effects of CYP11A1 siRNA and atorvastatin on cell viability, DU-145 cells seeded in 12-well plates were directly counted using Scepter handheld automated cell counter (Millipore, Billerica, MA, USA).

2.8. Immunofluorescence and visualization of actin filament

The cells attached to coverslips in 24-well plates were fixed with 2% paraformaldehyde (Nacalai Tesque) at room temperature for 30 min. The cells were then washed with PBS and permeabilized with 0.1% Triton-X-100 (Thermo Fisher Scientific) for 15 min. After washing thrice with PBS, the cells were blocked with 2% bovine serum albumin (Fujifilm Wako Pure Chemical) for 15 min. The cells were simultaneously probed with anti-E-cadherin rabbit monoclonal antibody (1:200 dilution, 24E10; Cell Signaling Technology) and anti-vimentin mouse monoclonal antibody (1:200 dilution, 5G3F10; Cell Signaling Technology) at 37 °C for 1 h. After washing with PBS, coverslips were incubated with CF®488A goat anti-rabbit IgG (1:200 dilution; Biotium, Hayward, CA, USA) and CF®568 goat anti-mouse IgG (1:200 dilution; Biotium) antibodies in the dark for 15 min. The cells were washed with PBS and incubated with Hoechst 33342 (5 μg/mL; Nacalai Tesque) for 15 min to stain the nuclei. After washing thrice with PBS, the cells were mounted on Fluoromount/Plus (Diagnostic Biosystems). Images were obtained using a 60× oil immersion objective lens on FluoView FV10i laser-scanning confocal microscope (Olympus).

Acti-stain 488 phalloidin (Cytoskeleton Inc., Denver, CO, USA) was used to visualize actin filaments (F-actin). Cell culture, fixation, permeabilization, and blocking were performed in the same way as described above. After washing with PBS, the cells were incubated with 0.1 μM phalloidin for 1 h, washed with PBS, and stained with 5 μg/mL Hoechst 33342 for 15 min. The coverslips were mounted on Fluoromount/Plus, and images were captured as described above.

2.9. Wound healing assay

Cells were seeded in 96-well plates at a density of 3.0×10^5 cells/mL to prepare a confluent monolayer. After attachment to the bottom of the plates, wounds were created using a P200 pipette tip. The medium was then replaced with FBS/antibiotic-free RPMI 1640, including atorvastatin and ketoconazole. Wound areas were photographed every 12 h after drug treatment for up to 36 h and measured using the ImageJ software.

For the siRNA experiments, cells (6.0×10^4 cells/mL) were transfected with siRNAs in 96-well plates as mentioned above. After being grown to nearly confluent, wounds were created using a P200 pipette tip. The cells were treated with atorvastatin and siRNAs in FBS/antibiotic-free medium. The wound areas were photographed and measured every 12 h after atorvastatin treatment.

2.10. Statistical analyses

Statistical analyses were performed using Excel Statistics 2016 for Windows (version 3.21; SSRI, Tokyo, Japan). Values were compared using the Student's two-tailed *t*-test and one-way ANOVA, followed by Dunnett *post-hoc* or Bonferroni *post-hoc* tests. The significance threshold for p-values was 0.05.

3. Results

3.1. CYP11A1 silencing suppressed the mevalonate pathway via cholesterol accumulation in DU-145 cells

CYP11A1 mRNA levels significantly decreased in CYP11A1 siRNA-transfected cells after 72 h ($p < 0.01$) (Fig. 1A, Supplementary Fig. S1A). As expected, intracellular free cholesterol significantly increased in the CYP11A1 siRNA-treated group compared to the control in CRPC cell line DU-145 previously defined as statin-resistant ($p < 0.05$) (Fig. 1D).[3,25] Similar effects were observed using Filipin III staining to detect intracellular cholesterol (Supplementary Fig. S2). Furthermore, mRNA expression of both HMGCR and HMG-CoA synthase 1 (HMGCS1) was reduced in CYP11A1 siRNA-treated cells (Fig. 1B and C). We performed the same analyses using another prostate cancer cell line, LNCaP (hormone-sensitive, statin-resistant), which could also synthesize androgens from cholesterol.[9,22,25–27] However, CYP11A1 silencing did not cause cholesterol accumulation or downregulation of HMGCR or HMGCS1 in LNCaP (Supplementary Fig. S1B–D).

3.2. CYP11A1 silencing sensitized DU-145 cells to atorvastatin

Atorvastatin reduced the viability of DU-145 and LNCaP cells in a dose-dependent manner (Fig. 2, Supplementary Fig. S3). In DU-145 cells, higher growth inhibitory effect of atorvastatin was observed in the CYP11A1 siRNA group than in the scrambled siRNA group, along with a decrease in atorvastatin IC_{50} (Fig. 2). Similar results were obtained using direct cell counting (Supplementary Fig. S4). In contrast, CYP11A1 silencing did not affect the impact of atorvastatin on LNCaP cells (Supplementary Fig. S3). These observations imply that responsiveness to CYP11A1 silencing varies across cell lines.

3.3. CYP11A1 silencing suppressed SREBP2-mediated feedback loop in DU-145 cells

We assessed the expression levels of active form of SREBP2, a transcription factor related to the mevalonate pathway, and its target gene after atorvastatin treatment in the presence and absence of CYP11A1 siRNA. Atorvastatin increased the expression of mRNA and active form of SREPB2 in a dose-dependent manner, which was weakened in the presence of CYP11A1 siRNA (Fig. 3A and B). Consistently, statin-induced upregulation of the SREBP2 target genes HMGCR, HMGCS1, and insulin induced gene 1 (INSIG1) was also attenuated by CYP11A1 siRNA (Fig. 3C–E).[28,29] Similarly, CYP11A1 siRNA suppressed atorvastatin-induced HMGCR protein expression (Fig. 3A).

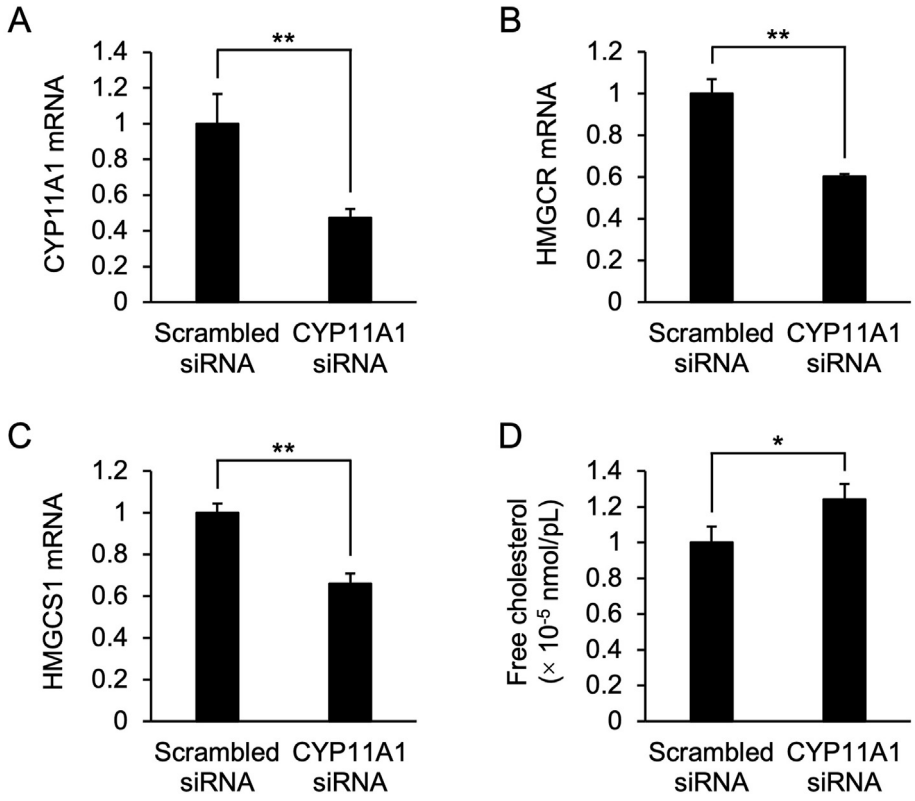

Fig. 1. Effects of CYP11A1 silencing on cholesterol content and mevalonate pathway-related gene expression in the CRPC cell line DU-145. (A–C) Effect of siRNA treatment on the mRNA expression of (A) CYP11A1, (B) HMGCR, and (C) HMGCS1. Cells were transfected with scrambled or CYP11A1 siRNA for 72 h. mRNA levels were determined using RT-qPCR. Data were normalized to RPLP1 mRNA levels in each sample and shown as relative values to the control. (D) Effect of CYP11A1 siRNA on free cholesterol content. Cholesterol was extracted from cells 72 h after siRNA transfection. Free cholesterol was measured using a colorimetric method. Each value is presented as mean ± SD (n = 3). Data were compared using the Student's two-tailed *t*-test. *p < 0.05, **p < 0.01.

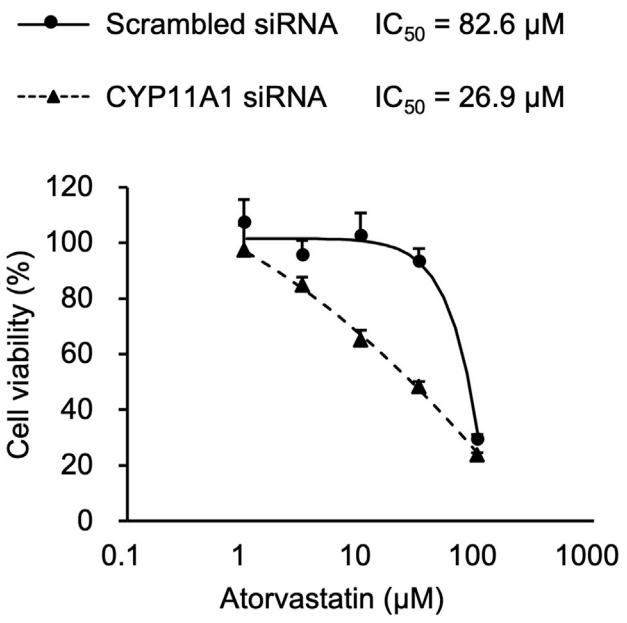

Fig. 2. Effect of CYP11A1 silencing on growth inhibitory effect of atorvastatin in DU-145 cells. Cell viability and IC_{50} values were determined using the CCK-8 assay in DU-145 cells after 72 h of atorvastatin treatment with siRNA transfection. Data represent mean ± SD (n = 5). Each value is expressed as a ratio relative to the vehicle control group (100%) in the scrambled or CYP11A1 siRNA group. Data were fitted to a dose-response curve using the ImageJ software to determine IC_{50} values.

3.4. CYP11A1 silencing induced EMT in DU-145 cells

Mesenchymal-like morphological changes, such as an increase in spindle cells and a decrease in cell-cell adhesion, were observed in CYP11A1 siRNA-treated DU-145 cells (Fig. 4A, Supplementary Fig. S5). To clarify whether CYP11A1 silencing induces EMT, we analyzed the expression of EMT marker molecules. The expression of E-cadherin, an epithelial marker, did not change at the transcriptional level, but decreased at the translational level (Fig. 4B and C, Supplementary Fig. S6A). The expression levels of the mesenchymal markers vimentin and fibronectin were elevated at both transcriptional and translational levels (Fig. 4B and C, Supplementary Fig. S6B and C). Furthermore, the subcellular localization of E-cadherin and vimentin was examined. E-cadherin was localized on the cell surface, especially between cells, in scrambled siRNA-treated cells. In contrast, E-cadherin signals on the cell surface were obscured due to reduced cell adhesion in CYP11A1 siRNA-treated cells (Fig. 4D). Inconsistent with the induction of EMT, CYP11A1 siRNA decreased the migration of DU-145 cells, even when used alone (Supplementary Fig. S7). The combination of CYP11A1 siRNA and atorvastatin most potently inhibited cell migration (Supplementary Fig. S7).

3.5. Some CYP11A1 inhibitors sensitized DU-145 cells to atorvastatin

Finally, we assessed whether CYP11A1 inhibitors sensitize DU-145 cells to atorvastatin using ketoconazole, mitotane, and aminoglutethimide.[30–33] Ketoconazole and mitotane alone reduced

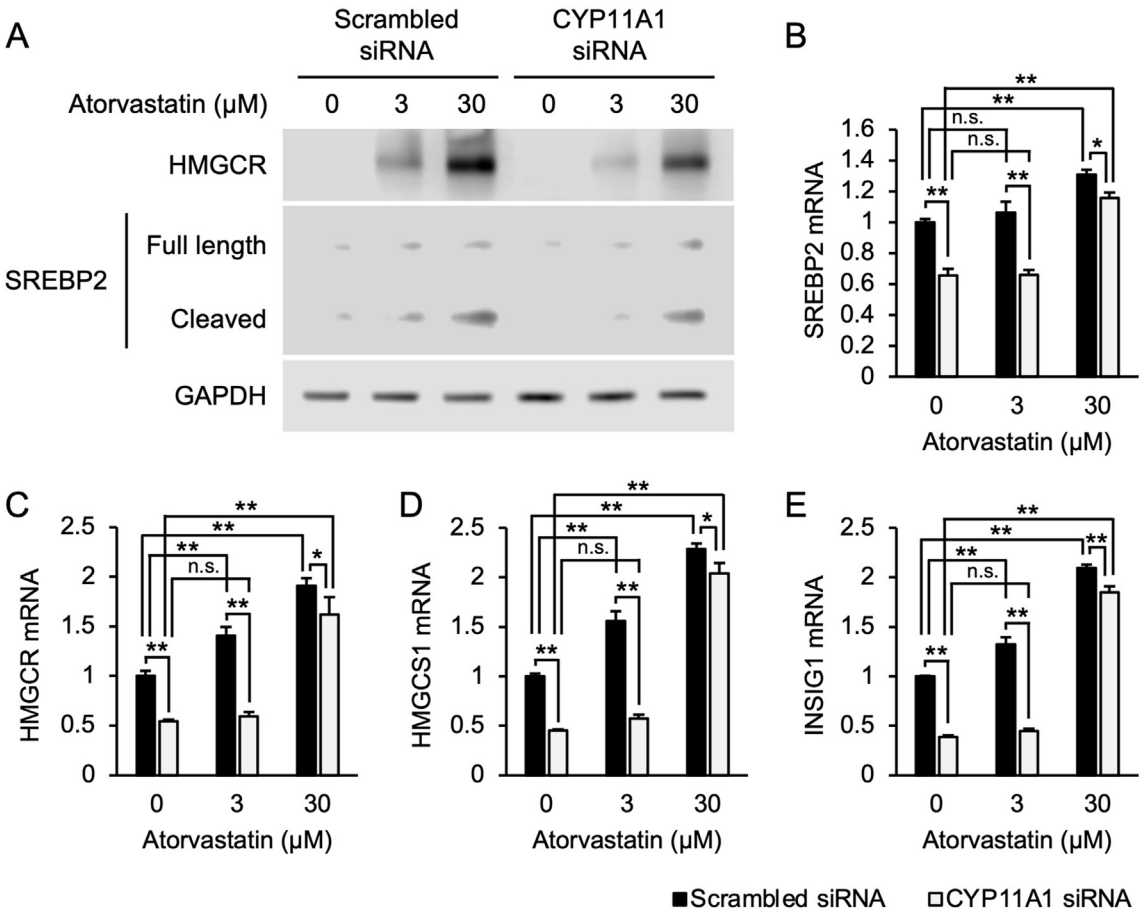

Fig. 3. Effect of CYP11A1 siRNA on feedback loop mediated by SREBP2 in DU-145 cells. (A) HMGCR and SREBP2 protein levels in DU-145 cells treated with siRNA and atorvastatin for 72 h were determined by Western blot analysis. GAPDH protein expression was used as the loading control. mRNA expression levels of (B) SREBP2 and SREBP2 target genes, (C) HMGCR, (D) HMGCS1, and (E) INSIG1 were measured using real-time PCR. Data were standardized to RPLP1 mRNA levels and expressed as relative to the scrambled siRNA-treated vehicle control group. Values represent mean ± SD (n = 3). Each group was analyzed using Bonferroni *post-hoc* test. n.s., not significant; *p < 0.05, **p < 0.01.

cell viability in a dose-dependent manner (Supplementary Fig. S8A and B). Moreover, cell growth was more potently inhibited by ketoconazole or mitotane in the presence of atorvastatin (Supplementary Fig. S8A and B). In contrast, aminoglutethimide had slight effect on cell viability, regardless of atorvastatin treatment (Supplementary Fig. S8C). Consistently, ketoconazole enhanced the growth inhibitory effect of 30 μM atorvastatin and significantly decreased atorvastatin IC_{50} ($p < 0.01$) (Fig. 5). In contrast, atorvastatin IC_{50} was not altered significantly by mitotane, although mitotane slightly enhanced the effect of 30 μM atorvastatin (Fig. 5). We evaluated the effects of ketoconazole and atorvastatin on cell migration in DU-145. The combination of ketoconazole and atorvastatin markedly inhibited cell migration, but did not significantly inhibit cell migration when used alone (Supplementary Fig. S9).

3.6. CYP11A1 inhibitors did not suppress SREBP2-mediated feedback loop in DU-145 cells

Furthermore, we investigated whether ketoconazole and mitotane inhibits SREBP2 expression. Contrary to our prediction, ketoconazole increased the expression of the active form of SREBP2 in the presence and absence of atorvastatin (Fig. 6A). Interestingly, ketoconazole alone increased the mRNA expression levels of HMGCR and HMGCS1 but did not affect them in the presence of atorvastatin (Fig. 6D and E). Similarly, atorvastatin-induced upregulation of HMGCR protein was slightly attenuated by ketoconazole, although ketoconazole alone induced HMGCR protein expression (Fig. 6A and B). Although mitotane did not affect the cleavage of SREBP2, it inhibited the mRNA expression of HMGCR, HMGCS1, and SREBP2 in the presence and absence of atorvastatin (Fig. 6A, C–E). Inconsistent with this data, mitotane enhanced atorvastatin-induced upregulation of HMGCR protein (Fig. 6A and B).

4. Discussion

In recent years, studies have anticipated the use of statins in cancer treatment because of novel findings suggesting their anticancer effect.[1] On the other hand, some cancer cells are resistant to statins due to their ability to induce HMGCR and mevalonate pathway-related genes, which remains an important issue.[6–9] We previously reported that inhibition of HMGCR expression with siRNA could sensitize statin-resistant cancer cells to statins, which could be an effective approach to overcome statin resistance in cancer cells.[10,11] In this study, we demonstrated that blocking the conversion of cholesterol into pregnenolone during steroidogenesis inhibited HMGCR expression and sensitized cells to statins in the statin-resistant CRPC cell line DU-145. We also suggested that downregulation of HMGCR could be caused by accumulation of intracellular free cholesterol. Xu *et al.* (2018) reported that inhibition of steroidogenesis with aminoglutethimide suppressed SREBP2 target gene expression, including HMGCR, in luteinized

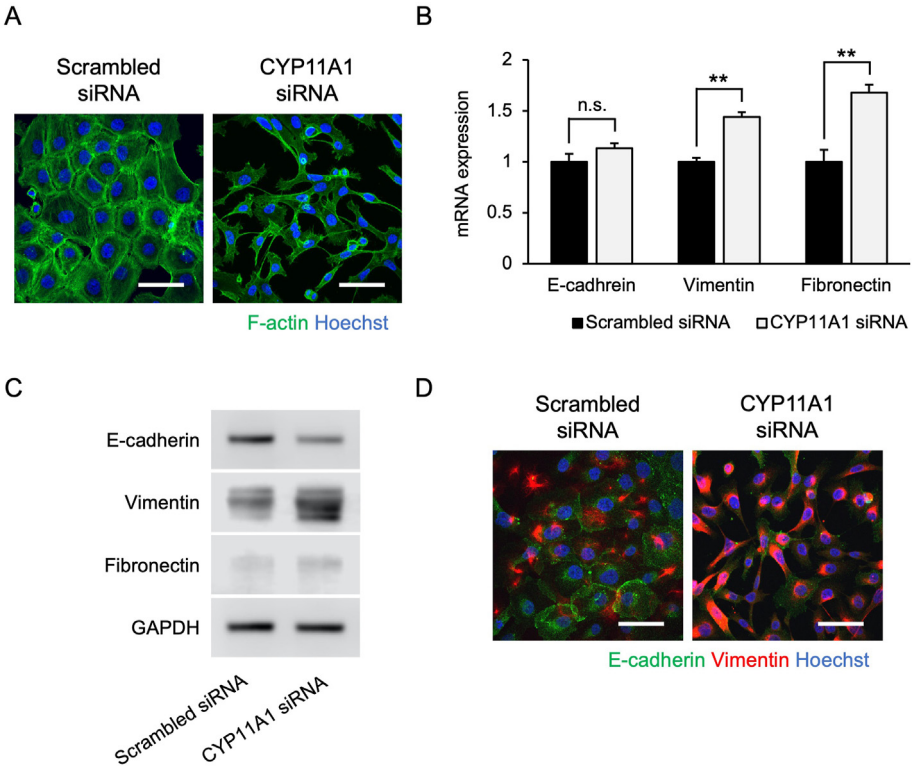

Fig. 4. CYP11A1 silencing induced EMT in DU-145 cells. (A) Merged images of siRNA-treated DU-145 stained with phalloidin (green, F-actin) and Hoechst (blue, nucleus). Cells were transfected with CYP11A1 siRNA or scrambled siRNA for 72 h before analysis. Scale bar = 50 μm. (B) Relative mRNA levels of E-cadherin, vimentin, and fibronectin were determined by RT-qPCR. Data were normalized to RPLP1 mRNA levels and compared by the Student's two-tailed *t*-test. Mean ± SD (n = 3). n.s., not significant; **p < 0.01. (C) Western blot analyses were performed to detect protein levels of E-cadherin, vimentin, and fibronectin. GAPDH protein level was used as the internal control. (D) Merged images of siRNA-transfected cells immunostained for E-cadherin (green), vimentin (red), and Hoechst (blue). Scale bar = 50 μm. (For interpretation of the references to color in this figure legend, the reader is referred to the Web version of this article.)

granulosa cells.[34] Furthermore, other researchers have indicated that the knockdown of SF-1, a transcription factor of CYP11A1, caused intracellular cholesterol accumulation with a decrease in CYP11A1 expression, although HMGCR mRNA level was not significantly altered in Leydig cells.[35] These findings suggest that cells with active steroidogenesis are likely to be affected by CYP11A1 inhibition.

SREBP2, a major regulator of cholesterol metabolism, regulates the expression of key enzymes involved in the mevalonate pathway, including HMGCR.[28] Longo *et al.* (2019) suggested that increased expression of genes related to sterol metabolism through statin-induced SREBP2 activation was involved in fluvastatin sensitivity in prostate cancer cell lines.[9] SREBP2 activation is inhibited by cholesterol and oxysterol.[15] In ovarian cancer cell lines, exogenous 25-hydroxycholesterol (25-HC) suppressed SREBP2 protein levels and expression of its target genes, resulting in increase in simvastatin-induced cell death.[36] Furthermore, 25-HC inhibited fluvastatin-induced increase in HMGCR mRNA expression and potentiated the cytotoxic effects of fluvastatin in prostate cancer cell lines.[9] In this study, we showed that CYP11A1 silencing suppressed statin-induced upregulation and activation of SREBP2, with an increase in intracellular free cholesterol in the CRPC cell line DU-145. This indicates that CYP11A1 inhibitors may act as indirect SREBP2 inhibitors by accumulating endogenous free cholesterol in CRPC cells.

Metastasis accounts for 90% of cancer-related deaths and is an important event in malignant progression of cancer.[37,38] During metastasis, the following key processes occur: local invasion, intravasation, circulation, extravasation, and colonization.[37,38] EMT contributes to some of these processes by increasing the motility, invasive potential, and stress resistance of epithelial cells.[16,37,38] Although EMT is associated with multiple drug resistance, atorvastatin has been reported to potently inhibit cell growth in epithelial cancer cells undergoing EMT.[11,17] Current data indicate that CYP11A1 silencing induces EMT and sensitizes cells to atorvastatin in the CRPC cell line DU-145, emphasizing the relationship between EMT and statin-sensitive phenotype. A previous study suggested that cholesterol induced EMT by inhibiting EGFR degradation in prostate cancer cells.[39] In present study, EMT induced by CYP11A1 silencing could be caused by an increase in free cholesterol. Recent studies have shown that EMT is associated with metabolic reprogramming including lipid metabolism.[40] In addition, we previously reported that the induction of EMT by TGF-β weakens statin-induced upregulation of HMGCR in an epithelial lung cancer cell line.[11] In this study, suppression of HMGCR induction was concurrent with EMT in cells transfected with CYP11A1 siRNA. This inhibition may also be attributed to the metabolic alterations associated with EMT.

In addition to the benefits of CYP11A1 inhibition in combination with statins, we demonstrated that CYP11A1 inhibition can contribute to malignant transformation via induction of EMT in CRPC. Several *in vitro* studies have demonstrated anti-metastatic effects of statins, including inhibition of migration, invasion, and EMT in prostate cancer cells.[41–43] The current study showed that CYP11A1 silencing inhibited cell migration in DU-145 cells. Furthermore, potent inhibitory effects were observed when combined with atorvastatin. This suggests that the combination of CYP11A1 inhibition and atorvastatin can effectively inhibit not only

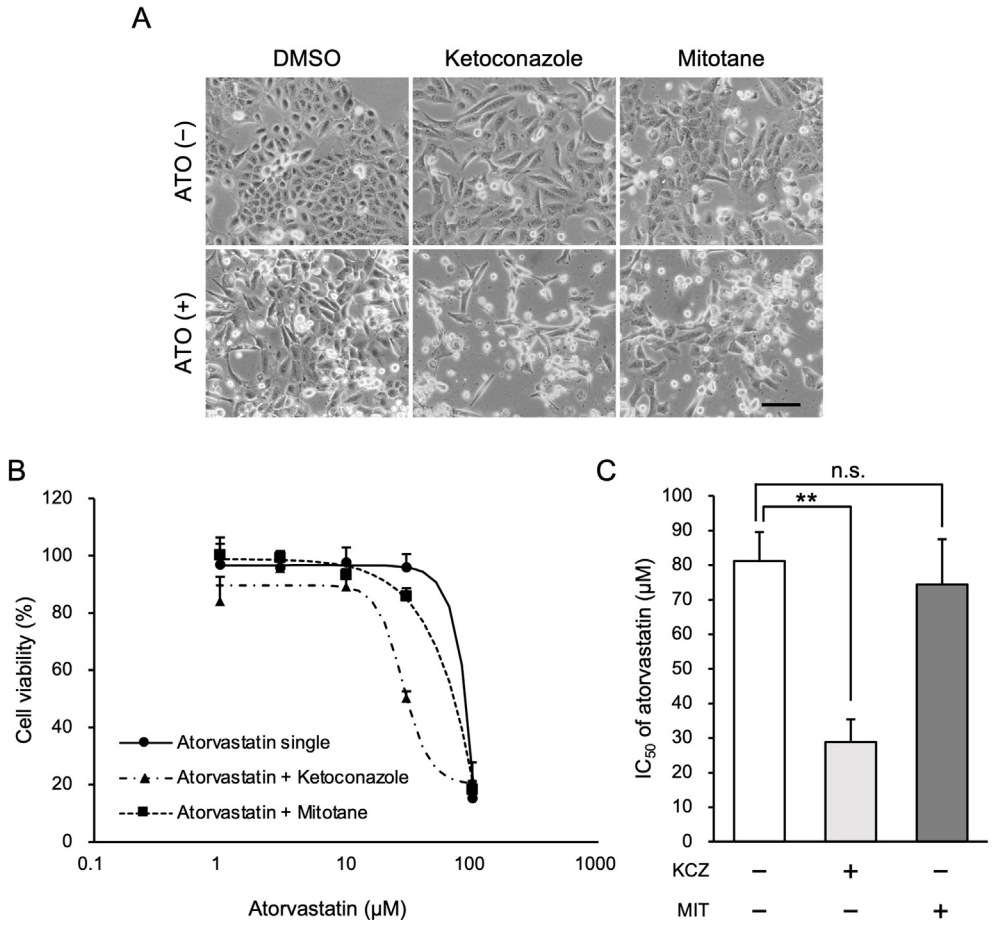

Fig. 5. Effects of CYP11A1 inhibitors on growth inhibitory effect and IC_{50} of atorvastatin. (A) Phase contrast image of DU-145 cells treated with 30 μM atorvastatin alone or in combination with 40 μM ketoconazole or 60 μM mitotane for 72 h. Scale bar = 100 μm (B) Cell viability was measured using the CCK-8 assay after 72 h of exposure to atorvastatin and 40 μM ketoconazole or 60 μM mitotane. Values were fitted to the concentration-response curve. Data represent mean ± SD (n = 5). (C) Atorvastatin IC_{50} was determined using the curve. Each group was analyzed using Dunnett's *post-hoc* test. Mean ± SD (n = 3). n.s., not significant; **p < 0.01. ATO, atorvastatin; KCZ, ketoconazole; MIT, mitotane.

cell growth but also cell motility in CRPC, although further investigation is required to elucidate whether the combination of CYP11A1 inhibition and statins suppresses cancer metastasis.

As mentioned above, aminoglutethimide treatment suppressed mRNA expression of SREBP2 and its target genes in luteinized granulosa cells.[34] Mitotane has also been reported to downregulate HMGCR mRNA expression and increase free cholesterol levels in adrenocortical carcinoma cells.[44] Therefore, we hypothesized that similar to CYP11A1 silencing, these agents might potentiate the anticancer effects of statins. However, neither aminoglutethimide nor mitotane significantly enhanced the effects of atorvastatin. These results indicated that the effects of these agents may depend on the cell type. Interestingly, we found that ketoconazole could sensitize the CRPC cell line DU-145 to atorvastatin. However, unlike CYP11A1 silencing, ketoconazole did not suppress SREBP2 activation. This implied that the sensitization effect to atorvastatin by ketoconazole may not be attributed to inhibition of CYP11A1. Ketoconazole, an inhibitor of CYP51A1, blocks the conversion of lanosterol, an intermediary metabolite in the mevalonate pathway.[45] Lanosterol accelerates HMGCR degradation without affecting SREBP2 activation.[15] Ketoconazole attenuated statin-induced upregulation of HMGCR protein, which may be ascribed to the degradation of HMGCR induced by accumulated lanosterol.

In conclusion, we demonstrated that the inhibition of CYP11A1 could sensitize CRPC cells to atorvastatin, suggesting that CYP11A1 inhibitors may be effective in combination with statins to overcome statin-resistant CRPC. Downregulation of HMGCR is a well-known effective approach for enhancing the anticancer effects of statins. For the first time, we speculate that this aim may be achieved by controlling the movement of metabolites related to the mevalonate pathway. This study has some notable limitations. First, androgen starvation treatment was not conducted in CYP11A1 silencing. Therefore, the effects of CYP11A1 inhibition may vary under these conditions. Second, CYP11A1 inhibition did not alter statin sensitivity in all the tested cell lines, suggesting a variation in responsiveness to CYP11A1 inhibition among the cell types. The reason for this has not yet been identified and requires further investigation. In addition, effect of atorvastatin itself on androgen synthesis was not investigated in this study although previous study revealed that simvastatin can affect some androgen synthesis enzyme expression and increase *de novo* androgen synthesis in CRPC cells.[46] Because an alteration of *de novo* androgen synthesis flow could directly affect intracellular cholesterol level, it is important to clarify effect of statins on gene expressions related to androgen synthesis. Moreover, only non-specific CYP11A1 inhibitors were used in this study, and a specific inhibitor was not tested. Some discordance in the molecular events between the experiments using siRNA and inhibitors may be attributed to the non-specific nature of the inhibitors. Finally, no *in vivo* experiments using animal models were performed. Further studies are needed to determine the practical applicability of CYP11A1 inhibitors and their enzyme specificity.

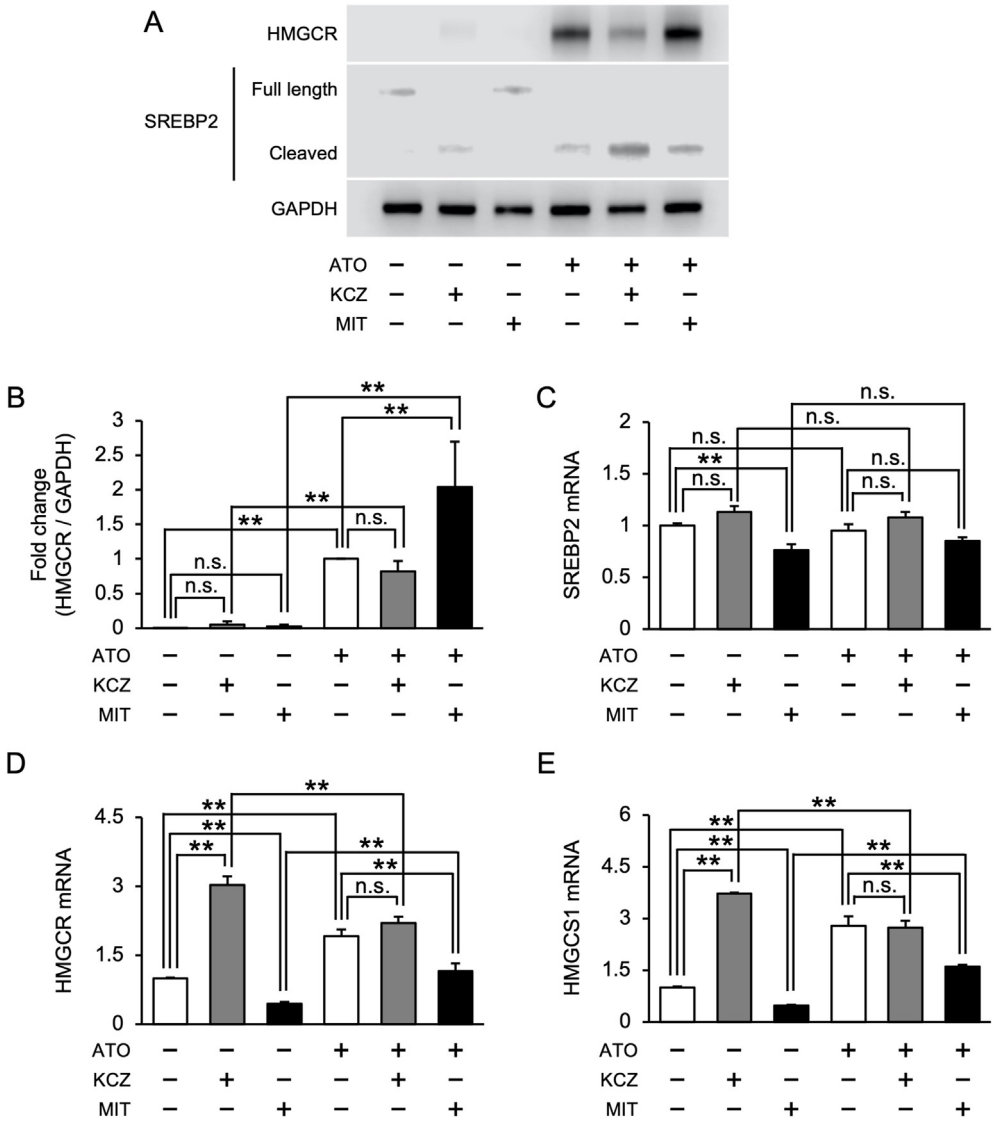

Fig. 6. Effects of CYP11A1 inhibitors on SREBP2-mediated feedback response. Cells were treated with 30 μM atorvastatin alone or in combination with 40 μM ketoconazole or 60 μM mitotane for 72 h before analysis. (A) Protein expression levels of HMGCR and SREPB2 were determined by Western blot analysis. GAPDH protein signal was used as the loading control. (B) Fold changes in HMGCR protein levels were quantified and normalized to GAPDH protein levels. The group treated with atorvastatin alone was set to 1. Mean ± SD (n = 3). (C–E) mRNA expression of (C) SREBP2, (D) HMGCR, and (E) HMGCS1 was measured by RT-qPCR. Each value was standardized to the RPLP1 mRNA levels and expressed relative to the vehicle control group. Each group was compared using Bonferroni *post-hoc* test. Mean ± SD (n = 3). n.s., not significant; **p < 0.01. ATO, atorvastatin; KCZ, ketoconazole; MIT, mitotane.

Author contributions

J.T. and K.W. designed the study. J.T. and A.S. performed the experiments. J.T., T.I., T.W., D.D.C., N.I., and K.W. analyzed the data. J.T., D.D.C., and K.W. wrote the manuscript. All authors read the manuscript and approved the final version.

Declaration of competing interests

The authors declare no conflict of interest.

Acknowledgements

This research was supported by the Japan Society for the Promotion of Science KAKENHI (grant number JP19H03514 to KW) through a Grant-in-Aid for Scientific Research (B).

Appendix A. Supplementary data

Supplementary data to this article can be found online at https://doi.org/10.1016/j.jphs.2023.08.002.

References

1. Joharatnam-Hogan N, Alexandre L, Yarmolinsky J, et al. Statins as potential chemoprevention or therapeutic agents in cancer: a model for evaluating repurposed drugs. *Curr Oncol Rep*. 2021;23:29. https://doi.org/10.1007/s11912-021-01023-z.
2. Pisanti S, Picardi P, Ciaglia E, D'Alessandro A, Bifulco M. Novel prospects of statins as therapeutic agents in cancer. *Pharmacol Res*. 2014;88:84–98. https://doi.org/10.1016/j.phrs.2014.06.013.
3. Warita K, Warita T, Beckwitt CH, et al. Statin-induced mevalonate pathway inhibition attenuates the growth of mesenchymal-like cancer cells that lack functional E-cadherin mediated cell cohesion. *Sci Rep*. 2014;4:7593. https://doi.org/10.1038/srep07593.
4. Raghu VK, Beckwitt CH, Warita K, Wells A, Benos PV, Oltvai ZN. Biomarker identification for statin sensitivity of cancer cell lines. *Biochem Biophys Res Commun*. 2018;495:659–665. https://doi.org/10.1016/j.bbrc.2017.11.065.

5. Yu R, Longo J, van Leeuwen JE, et al. Statin-induced cancer cell death can Be mechanistically uncoupled from prenylation of RAS family proteins. *Cancer Res*. 2018;78:1347–1357. https://doi.org/10.1158/0008-5472.CAN-17-1231.
6. Clendening JW, Pandyra A, Li Z, et al. Exploiting the mevalonate pathway to distinguish statin-sensitive multiple myeloma. *Blood*. 2010;115:4787–4797. https://doi.org/10.1182/blood-2009-07-230508.
7. Kimbung S, Lettiero B, Feldt M, Bosch A, Borgquist S. High expression of cholesterol biosynthesis genes is associated with resistance to statin treatment and inferior survival in breast cancer. *Oncotarget*. 2016;7:59640–59651. https://doi.org/10.18632/oncotarget.10746.
8. Göbel A, Breining D, Rauner M, Hofbauer LC, Rachner TD. Induction of 3-hydroxy-3-methylglutaryl-CoA reductase mediates statin resistance in breast cancer cells. *Cell Death Dis*. 2019;10:91. https://doi.org/10.1038/s41419-019-1322-x.
9. Longo J, Mullen PJ, Yu R, et al. An actionable sterol-regulated feedback loop modulates statin sensitivity in prostate cancer. *Mol Metabol*. 2019;25:119–130. https://doi.org/10.1016/j.molmet.2019.04.003.
10. Ishikawa T, Hosaka YZ, Beckwitt C, Wells A, Oltvai ZN, Warita K. Concomitant attenuation of HMG-CoA reductase expression potentiates the cancer cell growth-inhibitory effect of statins and expands their efficacy in tumor cells with epithelial characteristics. *Oncotarget*. 2018;9:29304–29315. https://doi.org/10.18632/oncotarget.25448.
11. Warita K, Ishikawa T, Sugiura A, et al. Concomitant attenuation of HMGCR expression and activity enhances the growth inhibitory effect of atorvastatin on TGF-β-treated epithelial cancer cells. *Sci Rep*. 2021;11:12763. https://doi.org/10.1038/s41598-021-91928-3.
12. Dong X-Y, Tang S-Q, Chen J-D. Dual functions of Insig proteins in cholesterol homeostasis. *Lipids Health Dis*. 2012;11:173. https://doi.org/10.1186/1476-511X-11-173.
13. Guerra B, Recio C, Aranda-Tavío H, Guerra-Rodríguez M, García-Castellano JM, Fernández-Pérez L. The mevalonate pathway, a metabolic target in cancer therapy. *Front Oncol*. 2021;11:626971. https://doi.org/10.3389/fonc.2021.626971.
14. Adams CM, Reitz J, Brabander JKD, et al. Cholesterol and 25-hydroxycholesterol inhibit activation of SREBPs by different mechanisms, both involving SCAP and Insigs. *J Biol Chem*. 2004;279:52772–52780. https://doi.org/10.1074/jbc.M410302200.
15. Song B-L, Javitt NB, DeBose-Boyd RA. Insig-mediated degradation of HMG CoA reductase stimulated by lanosterol, an intermediate in the synthesis of cholesterol. *Cell Metabol*. 2005;1:179–189. https://doi.org/10.1016/j.cmet.2005.01.001.
16. Islam MS, Morshedb MR, Babuc G, Khan MA. The role of inflammations and EMT in carcinogenesis. *Adv. Cancer Biol. Metastasis.*. 2022;5:100055 https://doi.org/10.1016/j.adcanc.2022.100055.
17. Rivas JDL, Brozovic A, Izraely S, Casas-Pais A, Witz IP, Figueroa A. Cancer drug resistance induced by EMT: novel therapeutic strategies. *Arch Toxicol*. 2021;95:2279–2297. https://doi.org/10.1007/s00204-021-03063-7.
18. Sung H, Ferlay J, Siegel RL, et al. Global cancer Statistics 2020: GLOBOCAN estimates of incidence and mortality worldwide for 36 cancers in 185 countries. *CA A Cancer J Clin*. 2021;71:209–249. https://doi.org/10.3322/caac.21660.
19. Vasaitis TS, Bruno RD, Njar VCO. CYP17 inhibitors for prostate cancer therapy. *J Steroid Biochem Mol Biol*. 2011;125:23–31. https://doi.org/10.1016/j.jsbmb.2010.11.005.
20. Feng Q, He B. Androgen receptor signaling in the development of castration-resistant prostate cancer. *Front Oncol*. 2019;9:858. https://doi.org/10.3389/fonc.2019.00858.
21. Twiddy AL, Leon CG, Wasan KM. Cholesterol as a potential target for castration-resistant prostate cancer. *Pharm Res (N Y)*. 2011;28:423–437. https://doi.org/10.1007/s11095-010-0210-y.
22. Bennett NC, Hooper JD, Lambie D, et al. Evidence for steroidogenic potential in human prostate cell lines and tissues. *Am J Pathol*. 2012;181:1078–1087. https://doi.org/10.1016/j.ajpath.2012.06.009.
23. Locke JA, Guns ES, Lubik AA, et al. Androgen levels increase by intratumoral *De novo* steroidogenesis during progression of castration-resistant prostate cancer. *Cancer Res*. 2008;68:6407–6415. https://doi.org/10.1158/0008-5472.CAN-07-5997.
24. Zhou J, Wang Y, Wu D, et al. Orphan nuclear receptors as regulators of intratumoral androgen biosynthesis in castration-resistant prostate cancer. *Oncogene*. 2021;40:2625–2634. https://doi.org/10.1038/s41388-021-01737-1.
25. Cattrini C, Capaia M, Boccardo F, Barboro P. Etoposide and topoisomerase II inhibition for aggressive prostate cancer: data from a translational study. *Cancer Treat Res Commun*. 2020;25:100221. https://doi.org/10.1016/j.ctarc.2020.100221.
26. Furuya Y, Sekine Y, Kato H, Miyazawa Y, Koike H, Suzuki K. Low-density lipoprotein receptors play an important role in the inhibition of prostate cancer cell proliferation by statins. *Prostate Int*. 2016;4:56–60. https://doi.org/10.1016/j.prnil.2016.02.003.
27. Kafka M, Gruber R, Neuwirt H, Ladurner M, Eder IE. Long-term treatment with simvastatin leads to reduced migration capacity of prostate cancer cells. *Biomedicines*. 2022;11:29. https://doi.org/10.3390/biomedicines11010029.
28. Xue L, Qi H, Zhang H, et al. Targeting SREBP-2-regulated mevalonate metabolism for cancer therapy. *Front Oncol*. 2020;10:1510. https://doi.org/10.3389/fonc.2020.01510.
29. Yabe D, Brown MS, Goldstein JL. Insig-2, a second endoplasmic reticulum protein that binds SCAP and blocks export of sterol regulatory element-binding proteins. *Proc Natl Acad Sci U S A*. 2002;99:12753–12758. https://doi.org/10.1073/pnas.162488899.
30. Fleseriu M, Castinetti F. Updates on the role of adrenal steroidogenesis inhibitors in Cushing's syndrome: a focus on novel therapies. *Pituitary*. 2016;19:643–653. https://doi.org/10.1007/s11102-016-0742-1.
31. Mast N, Linger M, Pikuleva IA. Inhibition and stimulation of activity of purified recombinant CYP11A1 by therapeutic agents. *Mol Cell Endocrinol*. 2013;371:100–106. https://doi.org/10.1016/j.mce.2012.10.013.
32. Kurokohchi K, Nishioka M, Ichikawa Y. Inhibition mechanism of reconstituted cytochrome P-450scc-linked monooxygenase system by antimycotic reagents and other inhibitors. *J Steroid Biochem Mol Biol*. 1992;42:287–292. https://doi.org/10.1016/0960-0760(92)90131-2.
33. Bossche HV. Inhibitors of P450-dependent steroid biosynthesis: from research to medical treatment. *J Steroid Biochem Mol Biol*. 1992;43:1003–1021. https://doi.org/10.1016/0960-0760(92)90328-G.
34. Xu Y, Hutchison SM, Hernández-Ledezma JJ, Bogan RL. Increased 27-hydroxycholesterol production during luteolysis may mediate the progressive decline in progesterone secretion. *Mol Hum Reprod*. 2018;24:2–13. https://doi.org/10.1093/molehr/gax061.
35. Hatano M, Migita T, Ohishi T, et al. SF-1 deficiency causes lipid accumulation in Leydig cells via suppression of STAR and CYP11A1. *Endocrine*. 2016;54:484–496. https://doi.org/10.1007/s12020-016-1043-1.
36. Casella C, Miller DH, Lynch K, Brodsky AS. Oxysterols synergize with statins by inhibiting SREBP-2 in ovarian cancer cells. *Gynecol Oncol*. 2014;135:333–341. https://doi.org/10.1016/j.ygyno.2014.08.015.
37. Fares J, Fares MY, Khachfe HH, Salhab HA, Fares Y. Molecular principles of metastasis: a hallmark of cancer revisited. *Signal Transduct Targeted Ther*. 2020;5:28. https://doi.org/10.1038/s41392-020-0134-x.
38. Zhuyan J, Chen M, Zhu T, et al. Critical steps to tumor metastasis: alterations of tumor microenvironment and extracellular matrix in the formation of pre-metastatic and metastatic niche. *Cell Biosci*. 2020;10:89. https://doi.org/10.1186/s13578-020-00453-9.
39. Jiang S, Wang X, Song D, et al. Cholesterol induces epithelial-to-mesenchymal transition of prostate cancer cells by suppressing degradation of EGFR through APMAP. *Cancer Res*. 2019;79:3063–3075. https://doi.org/10.1158/0008-5472.CAN-18-3295.
40. Sciacovelli M, Frezza C. Metabolic reprogramming and epithelial-to-mesenchymal transition in cancer. *FEBS J*. 2017;284:3132–3144. https://doi.org/10.1111/febs.14090.
41. Brown M, Hart C, Tawadros T, et al. The differential effects of statins on the metastatic behaviour of prostate cancer. *Br J Cancer*. 2012;106:1689–1696. https://doi.org/10.1038/bjc.2012.138.
42. Xie F, Liu J, Li C, Zhao Y. Simvastatin blocks TGF-β1-induced epithelial-mesenchymal transition in human prostate cancer cells. *Oncol Lett*. 2016;11:3377–3383. https://doi.org/10.3892/ol.2016.4404.
43. Zhu Z, Cao Y, Liu L, Zhao Z, Yin H, Wang H. Atorvastatin regulates the migration and invasion of prostate cancer through the epithelial-mesenchymal transformation and matrix metalloproteinase pathways. *Investig Clin Urol*. 2022;63:350–358. https://doi.org/10.4111/icu.20210411.
44. Boulate G, Amazit L, Naman A, et al. Potentiation of mitotane action by rosuvastatin: new insights for adrenocortical carcinoma management. *Int J Oncol*. 2019;54:2149–2156. https://doi.org/10.3892/ijo.2019.4770.
45. Stäubert C, Krakowsky R, Bhuiyan H, et al. Increased lanosterol turnover: a metabolic burden for daunorubicin-resistant leukemia cells. *Med Oncol*. 2016;33:6. https://doi.org/10.1007/s12032-015-0717-5.
46. Sekine Y, Nakayama H, Miyazawa Y, et al. Simvastatin in combination with meclofenamic acid inhibits the proliferation and migration of human prostate cancer PC-3 cells via an AKR1C3 mechanism. *Oncol Lett*. 2018;15:3167–3172. https://doi.org/10.3892/ol.2017.7721.